Electron Transfer in Platinum(II) Diimine-Centered Triads: Mechanistic Insights from Photoinduced Transient Displacement Current Measurements

James E. McGarrah,*,†,§ Joseph T. Hupp,† and Sergei N. Smirnov‡

Department of Chemistry, Northwestern University, Evanston, Illinois 60208, and Department of Chemistry, New Mexico State University, Las Cruces, New Mexico 88003-8001

The consequences of photoexcitation of a platinum diimine bisacetylide complex and its triads with phenothiazine species (McGarrah, J. E.; Eisenberg, R. *Inorg. Chem.* **2003**, *42*, 4355−4365) were investigated by the photoinduced transient displacement current (PTDC) method, with the aim of understanding the role of solvent in defining the nature and extent of intratriad electron transfer. PTDC enables reports on the distance of charge separation in photoexcited states. Photoexcition of the triad, $Pt(dbbpy)(CCC_6H_4CH_2(PTZ))_2$ (where dbbpy = 4,4′-di-*tert*-butyl-2,2′-bipyridine), leads to formation of the ^{3}MLCT excited state, which in CH_2Cl_2 is intramolecularly quenched by PTZ to form a charge-separated (CS) state, $Pt(dbbpy^{\cdot-})(CCC_6H_4CH_2(PTZ)CCC_6H_4CH_2(PTZ^{\cdot+})$; the CS state features a dipole moment oriented in essentially the opposite direction to that of the ground state. In toluene the last step of charge separation is shut down. In THF these two transient states are equilibrated, approximately as a 1:1 mixture of ^{3}MLCT and CS states, causing a complex, but instructive, PTDC response. The PTDC response for $Pt(dbbpy)(CCC_6H_5)_2$, on the other hand, is similar in all solvents and shows a negative signal corresponding to a long-lived, and comparatively nonpolar, ^{3}MLCT state. The ground-state dipole moment, μ_g, weakly increases with solvent polarity, from ∼11.5 D in toluene to ∼15.5 D in THF and CH_2Cl_2.

Introduction

The goal of mimicking the initial steps of photosynthesis is to capture visible light in order to separate charges and utilize the absorbed energy. The challenge is to design molecules where the photogenerated redox pair is separated efficiently and for a long enough time for electrical storage or chemical conversion of the captured energy to occur.[1–3] The resultant charge-separated (CS) state is most often studied by time-resolved transient absorption (TA) spectroscopy because of its high time resolution and ability to identify the moieties that have accepted or donated electrons. Nevertheless, detailed information about charge distribution in CS states is often difficult, if not impossible, to obtain by simple spectral difference measurements. Herein we apply the photoinduced transient displacement current (PTDC) technique[4] to the problem of photoinduced electron transfer within a representative platinum(II) diimine bisacetylide complex (**1**) and two of its triads (**1-PTZ** and **2-PTZ**) with phenothiazine species (electron donors).

The presence of a dipole moment is a direct indication of separated charges, with the magnitude of the dipole moment providing a measure of the distance between the separated charges. The PTDC technique measures the dipole moments of transient states formed created by a light pulse.[4–8] Importantly, both initially formed states and subsequently formed states can be examined. Thus, PTDC allows for direct observation and quantification of photoinduced inter- and intramolecular charge transfer.[9–12]

SCHEME 1: Processes and Their Labels for Photoexcited 1-PTZ
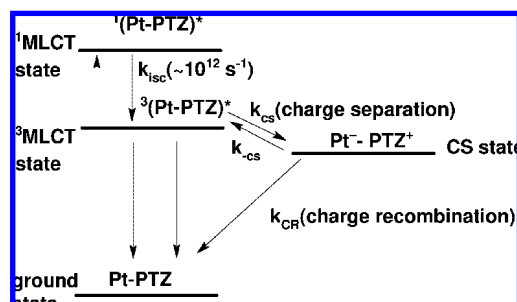
The photophysical behavior of **1** and its PTZ triads has previously been studied by picosecond transient absorption spectroscopy.[14] The lowest energy charge-transfer excited state of **1** had been described as an ^{3}MLCT (metal-to-ligand charge transfer), where diimine was the ligand involved in the charge transfer.[15–23] Recent studies have pointed out the limitations of such descriptions by drawing attention to admixing of acetylide π-orbitals in the HOMO of the Pt(II) diimine bisacetylide.[24,25] Nevertheless, we will use the above notation here and refer to the lowest energy excited state as ^{3}MLCT.

Excitation into the ^{1}MLCT band of **1** leads to formation of a ^{3}MLCT state within 200 ± 40 fs. The triplet is highly luminescent ($\phi_{lum} = 0.34 \pm 0.05$), with a lifetime $\tau_{lum} = 1.36$ μs in CH_2Cl_2 at room temperature.[24] **1-PTZ** and **2-PTZ** were designed as electron transfer triads (see Scheme 1), with the PTZ moiety reductively quenching the ^{3}MLCT state to produce a highly dipolar CS state. However, quenching and CS state formation in **1-PTZ** have been observed only in polar solvents such as acetonitrile.[14] Formation of CS state does not occur in nonpolar solvents such as toluene, reflecting their ineffectiveness

* To whom correspondence should be addressed. E-mail: mcgarrah@geneseo.com.
† Northwestern University.
‡ New Mexico State University.
§ Current address: SUNY at Geneseo, Chemistry Department, Geneseo, NY 14454.

Platinum(II) Diimine-Centered Triads

J. Phys. Chem. A, Vol. 113, No. 23, 2009 **6431**

in solvating and stabilizing highly polar states. The conclusions derived from luminescence studies of **1** and **1-PTZ** are further supported by transient absorption spectroscopy measurements in polar solvents, most notably the observation of the PTZ radical cation with a maximum near 520 nm.[14] Here we employ the PTDC technique to corroborate the interpretation, evaluate the time evolution of charge distributions, and elucidate the role of solvent in modulating charge separation.

Theory

We start by briefly reviewing the theoretical background for the PTDC technique. The theory has been described previously,[4–7,9,12] and here we reintroduce the key points that are important for understanding the technique and the data interpretation. The displacement current is measured as a voltage drop across a load resistor, R. In our case, it is the input resistance of the oscilloscope, $R = 50 \, \Omega$. The photoinduced voltage, v, is described by eq 1:

$$v + \tau_{RC}\frac{dv}{dt} = RS\frac{dP_{solute}}{dt} \qquad (1)$$

where τ_{RC} is the RC time constant of the circuit with C being the cell capacitance and S is the area of the electrodes. In the eq 1 the electric polarization due to solutes, P_{solute}:

$$P_{solute} = \sum_{solutes,i} n_i \langle u_i \rangle \qquad (2)$$

evolves because of two factors: the change of the dipole concentrations, n_i, and their reorientation. The latter is hidden in the average projection of the dipole moment $\langle u_i \rangle$, which is a function of time and the initial distribution. If molecular rotation, described by the rotational time, τ_r, is fast, the average dipole moment, $\langle u_i \rangle$, can be treated as if at quasiequilibrium, and eq 1 can be rewritten as:

$$v + \tau_{RC}\frac{dv}{dt} = \frac{RSV_0}{d}\sum_i \frac{\phi_{si}M_i^2}{3k_BT}\frac{dn_i}{dt} \qquad (3)$$

where k_B and T are the Boltzmann constant and temperature, respectively. The factor φ_{si} accounts for the local field on each dipole and the contribution from the solvent surrounding it. The dipole moments, M_i, are different from what they would be in the gas phase due to interaction with the solvent. Both these adjustments depend on the dielectric properties of the solvent, shape of the dipolar solute molecule, and its polarizability; the adjustments can be approximated differently depending on the relative size of the solute and solvent molecules. For large molecules, the most convenient approximation is to encase each solute dipole into a sphere together with some solvent molecules.[9,12] In the semicontinuum approximation, such extended 'molecules' have the local field factor, φ_s, dependent on only the dielectric constant, ε, and the refractive index, n_D, of the solvent:

$$\phi_s = \left(\frac{\varepsilon(2\varepsilon + n_D^2)}{2\varepsilon + 1}\right)^2 \frac{3}{2\varepsilon^2 + n_D^4} \qquad (4)$$

Due to the imposed spherical cavity, the net interaction of the solute dipole moment with remaining solvent outside the cavity is zero. The dipole moment, M_i, is then a sum of the solute dipole moment, μ'_i, and the induced dipole moment in the solvent, m_{si}, included into the sphere:

$$M_i = \mu'_i + m_{si}, \qquad (5)$$

Note that eqs 4 and 5 are not affected by the size of the sphere chosen, unlike in the Lippert–Mataga analysis of the fluorescence maximum shift with solvent polarity; thus, PTDC offers a more direct measure of dipole moments. The main contribution to M_i is from the solute dipole moment, μ'_i, which is usually the primary goal of such experiments, i.e., the measure of average distance, r_i, between the separated charges in the solute molecule:

$$\mu'_i = er_i, \qquad (6)$$

The dipole moment in solution, μ'_i, can be quite different from the gas-phase dipole moment, μ_i, because of polarizability and the solvent reaction field and can depend strongly on the solvent polarity. Nevertheless, the meaning of eq 6 remains the same: μ'_i provides the distance between the centers of positive and negative charges for a molecule in that solvent. The solvent contribution, m_s, to the total dipole moment results from solvent molecules oriented by the solute dipole. In a semicontinuum model, m_s can be calculated by integrating the electric polarization outside the molecular cavity. The latter can be approximated using the electric field, E_{vac}, from the charges placed in the molecular frame in accordance with the molecule's dipole moment.[9] Integration over the region occupied by solvent inside the spherical cavity, $V \neq V_s$, will produce the estimate for the solvent contribution to the dipole moment:

$$\vec{m}_s = \frac{\varepsilon - 1}{4\pi}\int_{V \neq V_s}\vec{E}(\vec{r})dV \approx \frac{\varepsilon - 1}{4\pi\varepsilon}\int_{V \neq V_s}\vec{E}_{vac}(\vec{r})dV \qquad (7)$$

The region of integration is constructed by 'rolling' a sphere over the molecular surface. The molecule is represented by a superposition of overlapping spheres with appropriate atomic van der Waals radii. The radius for a 'rolling' solvent molecule is taken such that its volume equals the van der Waals volume of the solvent molecule. These radii were calculated to be 2.8 Å, 2.5 Å, and 2.3 Å, for toluene, THF, and CH_2Cl_2, respectively.[9]

Equation 3 becomes incorrect when solute rotation is 'slow'. A more complicated analysis is required, but it allows the collection of more detailed information about the dipole moments of all states, which otherwise would be unavailable for $\tau_r = 0$. The solution to the problem is derived from evaluating a modified Debye equation,[6,7] eq 8, for the angular distribution functions, f_i, describing how the concentrations, n_i, of dipoles μ'_i with orientation in a solid angle $d\Omega_i$, change because of dipole rotation (via diffusional drift under the external field E) and because of conversion into/from other dipoles, μ'_j; the latter have their angular distribution functions f_j.

$$\frac{\partial f_i n_i}{\partial t} = \frac{n_i}{2\tau_r}\frac{\partial}{\partial \xi}\left(\left(\frac{\partial f_i}{\partial \xi} - \gamma_i E\right)(1 - \xi^2)\right) + \sum_{j \neq i}[f_j k_{ji} n_j - f_i k_{ij} n_i] \qquad (8)$$

Here ξ_i means the cosine of an angle between the dipole μ'_i and the external electric field, E; and k_{ij} is the rate constant for dipole μ'_i transition into μ'_j. The substitution $\gamma_i = \varphi_s\mu'_i/k_BT$ is introduced for convenience. The solution to eq 8 is provided elsewhere,[6,7] and we briefly reproduce it here. The angular distribution function, f_i, expanded in Legendre functions $P_l(\xi_i)$:

$$f_i = \frac{1}{2\pi}\left(1 + \sum_{l>0}a_i^l P_l(\xi_i)\right) \qquad (9)$$

allows transformation of eq 8 into the set of equations for coefficients a_i^l. Because the distribution functions f_i are only

slightly different from isotropic, high order coefficients with $l > 2$ in eq 9 are of diminishing importance, $a_i^{(1)} \sim (\mu'_i E/k_B T)^l$, and can be ignored. The polarization is given by $a_i^{(1)}$, but the initial condition for $a_i^{(2)} \sim 1$ (caused by the laser excitation) requires inclusion of the second order Legendre term, $a_i^{(2)}$, as well. For convenience, we will substitute $y_i = a_i^{(1)} n_i$ and $z_i = a_i^{(2)} n_i$, which results in the following set of equations:

$$
\begin{aligned}
\frac{dn_i}{dt} &= \sum_{j \neq i} [k_{ji} n_j - k_{ij} n_i] \\
\frac{dy_i}{dt} &= \left[-y_i + \gamma_i E \left(n_i - \frac{2z_i}{5} \right) \right]/\tau_r + \sum_{j \neq i} [k_{ji} \beta_{ij} y_j - k_{ij} y_i] \\
\frac{dz_i}{dt} &= -3z_i/\tau_r + \sum_{j \neq i} [k_{ji} z_j P_2(\beta_{ij}) - k_{ij} z_i]
\end{aligned}
$$

$$(10)$$

Here β_{ij} are the correlation factors, which are equal the cosine of an angle, θ_{ij}, between the dipoles μ'_i and μ'_j (in the molecular frame):

$$\beta_{ij} = \cos(\theta_{ij}) \qquad (11)$$

In the majority of cases the correlation factors are either $\beta_{ij} = 1$ or $\beta_{ij} = -1$, i.e., the dipoles lie along the same axis. Note that the rotational time, τ_r, is assumed to be the same for all states. This is a fairly good approximation, unless the solute size and/or interaction between solute and solvent changes dramatically upon excitation. The set of eqs 10 deals with three quantities: the concentrations, n_i, the average dipole orientation, y_i, and the second order of their distribution, z_i. The desired electrical polarization is given by y_i via:

$$P_{solute} = \phi_s \sum_{solutes, i} y_i M_i \qquad (12)$$

Thus, after calculating P_{solute} from eq 12 using y_i for all dipoles and the measured number of photons, one can substitute it into eq 1 to get the time variation of the dipole signal. Fitting the experimental signal with the calculated theoretical one, in which the values of the dipole moments, rotation time, and the rates of transitions are varied, should allow for the recovery of these values. The more parameters (states) involved, the more independent data is required. For cases with more than one excited state, the fitting of a photoresponse signal can be ambiguous, especially when its signal-to-noise ratio is not very high. Contribution of each state to the signal depends not only on its dipole moment but on all the preceding rate constants k_{ij}, the dipole moments of those states, and the rotation time, τ_r. In the limiting case of a very short τ_r, the signal would be uniquely defined only by the difference of the squared dipole moments, $M_e^2 - M_g^2$, between the ground, M_g, and (the final) excited state, M_e, and the lifetime of the latter. These simplifications make the fitting straightforward but provide no information on the individual dipole moments out of the $M_e^2 - M_g^2$ combination. Independent measure of M_g without excitation can help. Alternatively, nonzero rotation time allows discrimination between M_e and M_g, especially if the initial distribution of excited dipoles can be altered. The latter is achieved by varying the excitation light polarizations, perpendicular and parallel to the applied field, which will be used in this paper, as shown below. The approach provides an additional degree of freedom in measurements that allows better accuracy in determining the parameters by global fitting, i.e., fitting the signals of different light polarizations using the same set of parameters. When three (the ground and two excited) or more states are involved, an
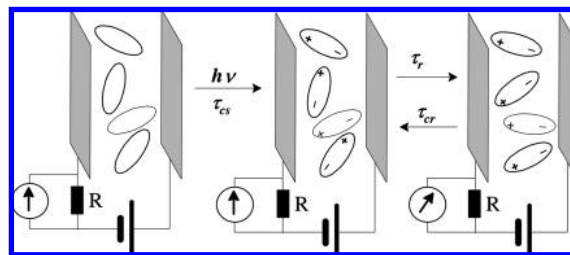

Figure 1. A diagram of the photoinduced transient displacement current experiment.

independent measure of the transition rates between different dipolar states, k_{ij}, is very helpful and can be obtained using transient absorption spectroscopy. Generally, it is difficult to justify a good accuracy for all fitted parameters in cases with more than three states, and, even for the latter, in many situations the information about the intermediate state is often lost, as will be discussed in the results.

1   **1-PTZ** (R = ^{t}Bu)   **2-PTZ** (R = CO$_2$Et)
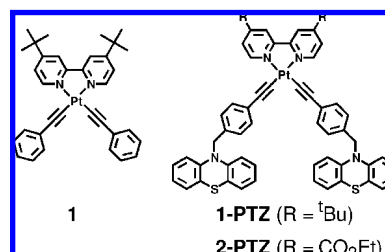
Experimental Section

Compounds **1**, **1-PTZ**, and **2-PTZ** were prepared as previously described.[14,15] Their purity was confirmed by ^{1}H NMR (400 MHz) and TLC. All solvents used were of spectroscopic grade and used without further purification.

Dipole Measurements. Figure 1 shows a schematic representation of the experimental setup. The solution of desired molecules ($\sim 10^{-4}$ M) in between two parallel stainless steel electrodes separated by a distance $d = 0.79$ mm and confined by two quartz windows, is excited with ~ 2 ns fwhm laser pulse at 420 nm from an Opotek Vibrant laser (Model 355 I). Polarization of light can be chosen either perpendicular or parallel to the applied electric field by a polarizer. The newly formed dipoles of the transient states reorient with a rotation time, τ_r, and tilt in the electric field from the applied voltage ($V_0 = 600-800$ V). The resulting transient displacement current signal is measured and digitized by a TDS 684A oscilloscope. The dipole signal fitting involved minimization of χ^2 between the experimental and the calculated traces using eqs 1, 10, and 12. The calculated signal was convoluted with the experimental laser pulse time profile recorded with a fast photodiode on the same oscilloscope. The profile was scaled using the number of absorbed photons measured from the incident and transmitted laser energy monitored during the experiment. The RC time, τ_{RC}, was calculated based on the cell dimensions and solvent dielectric constant; the quality of this calculation was confirmed by independent measurements.

The rotation times, τ_r, were obtained from the fittings when it was unambiguous, such as for **1** in all solvents and for **1-PTZ** in toluene. The values appear to scale well with the changes of solvent viscosities and volumes of the solutes. Thus, in order to minimize the number of variables for fitting signals of **1-PTZ** and **2-PTZ** in THF and CH$_2$Cl$_2$, the values of the corresponding τ_r were scaled according to the viscosity and volume change.
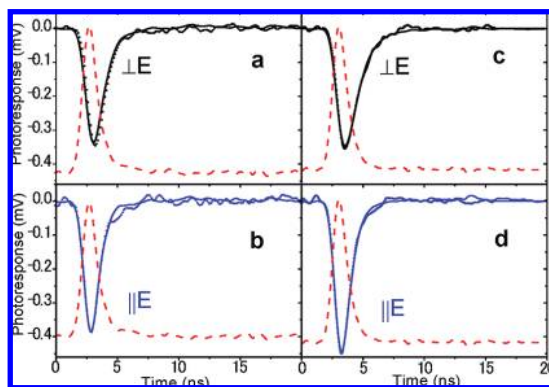
Platinum(II) Diimine-Centered Triads

J. Phys. Chem. A, Vol. 113, No. 23, 2009 **6433**

Figure 2. Photoresponses of **1** (**a** and **b**) and **1-PTZ** (**c** and **d**) in toluene at room temperature excited at 420 nm with the light polarization parallel (left) and perpendicular (right) to the applied electric field of 700 V across 0.79 mm gap. The dotted lines are the experimental photoresponses (scaled to 42 μJ of absorbed energy in all cases) and the red dashed line is the laser pulse time profile. The solid lines are the simulated data fittings with the parameters listed in Tables 1 and 2.

TABLE 1: PTDC Data for 1 in Different Solvents

solvent	M_g (D)	M_{MLCT} (D)	τ_{MLCT} (ns)	τ_r (ns)
CH_2Cl_2	15.5 ± 2	$0 - 3$	>100	0.3 ± 0.1
THF	15.5 ± 0.9	$0 - 3$	>100	0.35 ± 0.1
toluene	11.4 ± 0.8	$0 - 3$	>100	0.4 ± 0.1

Results and Discussion

In the present study nonpolar toluene and moderately polar THF and CH_2Cl_2 were used as solvents for studying the PTDC photoresponse. Higher polarity solvents were excluded because of significant 'dark current', which makes it difficult to use PTDC with steady applied voltage. As it will be seen, the range of dielectric constants, from $\varepsilon = 2.3$ to $\varepsilon = 8.9$, appeared sufficient to significantly vary the relative energies of MLCT and CS states in **1**, **1-PTZ**, and **2-PTZ**.

All three studied molecules possess nonzero dipole moments in the ground state that diminish to almost zero upon excitation to the rapidly formed ^{3}MLCT state.[26] Figure 2 shows the PTDC photoresponses for **1** and **1-PTZ** in toluene. In both samples the signal is negative, which indicates a ground state that is more polar than the excited state, an expected result based on the observed negative solvatochromism for these compounds. Excitation at 420 nm is at the ^{1}MLCT band and the transition moment is aligned with the ground-state dipole moment. Consequently, the dipole signal evolution is faster for light polarization parallel (∥) to the electric field (the dipoles are already prealigned) than for the perpendicular polarization (⊥). The difference between the signals for the two light polarizations is clearly visible and is due to the rotation times, $\tau_r = 0.4 \pm 0.1$ ns and 0.6 ± 0.1 ns, for the two molecules, respectively, being longer than the setup time resolution. The values are in reasonable agreement with the simple estimate of the hydrodynamic model for the rotational relaxation time of a spherical object in a solvent of viscosity η:[27]

$$\tau_{r\_sph} = \frac{V\eta}{k_B T} \tag{13}$$

For a sphere with the volume of **1** (3100 Å^3)[28] and the triad **1-PTZ** (4800 Å^3) the rotation times in a solvent of the toluene viscosity, $\eta(25\ °C) = 0.56$ mPa·s,[30] one estimates $\tau_{r\_sph} = 0.43$ and 0.67 ns, respectively.

The ^{3}MLCT state is quite long-lived, and thus the state appears as an inconspicuous positive part of the signals,

**TABLE 2: PTDC Data for 1-PTZ in Different Solvents**

solvent	M_g (D)	M_{MLCT} (D)	M_{CS} (D)	τ_r (ns)	τ_{CS} (ns)	τ_{CR} (ns)
CH_2Cl_2	≤ 14	≤ 5	44 ± 2	0.4 ± 0.1	0.5 ± 0.2	8 ± 3
THF	11 ± 1	$0 - 3$	21 ± 1^a	0.45 ± 0.1	0.6 ± 0.1^a	8 ± 1
toluene	12 ± 0.8	$0 - 3$	^{b}	0.6 ± 0.1	$>100^b$	

^{a} The data in THF can be alternatively interpreted as equilibrium between ^{3}MLCT and CS states. See text for details. ^{b} No measurable formation of CS state was observed in toluene.

indistinguishable from the baseline. No suitable fit to the data (i.e., for both light polarizations with the same set of parameters) can be obtained for $M_{MLCT} > 5$ D or $M_{MLCT} < -2$ D (as if $M_{MLCT} = 2$ D is pointing in the opposite direction to M_g). Variation within the range -2 D $< M_{MLCT} < 5$ D, on the other hand, practically does not affect the value of M_g (less than 5% difference) and results in the ground-state dipole moments of **1** and **1-PTZ** in toluene $M_g = 11.4 \pm 0.8$ D and 11.9 ± 0.8 D, respectively. The above-mentioned best-fit rotation times are also listed in Tables 1 and 2. Both dipole moment values, M_{MLCT} and M_g, are in a good agreement with the simple view of the formal charges of the ligands and the Pt ion in the ground and excited states. Using the molecular geometry taken from X-ray structural measurements,[31] and by placing +2 charge on Pt while assigning negative charges to each metal bound carbon of the acetylides, one obtains $\mu'_g = 13.2$ D. This value reduces to $M_g = 11.4$ D in toluene; the same charge distribution would correspond to $M_g = 10.4$ and 10.3 D in THF and CH_2Cl_2, respectively.[32] Similarly constructed charge distribution in the excited MLCT state with Pt having +3 charge and an additional negative charge on bpy, with the presumption of unaltered molecular geometry, gives $\mu'_{MLCT} = 2.5$ D collinear with that of the ground state. This dipole moment changes to $M_{MLCT} = 2.3$ and 2.2 D, when the molecule is placed in toluene and THF/CH_2Cl_2, respectively.[32] Castellano and co-workers have calculated a similar value for μ'_g of 10.6 D by DFT in the gas phase.[24,25] A comparable ground-state dipole moment was measured by VanHelmot and Hupp on a related platinum containing chromophore, Pt(dpphen)(ecda) (where dpphen is 4,7-diphenyl-1,10-phenanthroline and ecda is 1-(ethoxycarbonyl)-1-cyanoethylene-2,2′-dithiolate), also by using the PTDC method.[33]

The dipole signal of **1** in solvents of different polarities moderately changes. The apparent M_g slightly increases in THF and CH_2Cl_2, to $M_g = 15.5 \pm 2$ D (see Table 1). Note that this increase occurs despite the enhanced negative solvent contribution (m_s) and thus illustrates a noticeable polarizability of the ground state: the value of $M_g = 15.5$ D translates to μ'_g on the order of 20 D in these solvents. Alternatively, it may point to limitations of the semicontinuum approximation in calculating the solvent contribution to the dipole moments, m_s. The rotation times should shorten in these solvents due to the lower viscosities of THF and CH_2Cl_2, but the experimental accuracy for obtaining their values declines due to a greater contribution of $\tau_{RC} > \tau_r$ to the signal broadening in these polar solvents. Experimentally we can only provide the upper limit for τ_r in such cases, as both times (τ_{RC} and τ_r) contribute to the broadening almost identically.[4,5]

The dipole signal evolution is quite different for **1-PTZ**, where the PTZ moiety can reductively quench the ^{3}MLCT state by intramolecular charge transfer.[14] Increased solvent polarity provides sufficient solvation for the CS state to make it of a lower energy than the ^{3}MLCT state and allow charge transfer from PTZ to Pt to occur. The dipole signal of **1-PTZ** in CH_2Cl_2

SCHEME 2: Illustration of Location for Effective Charges in Different States of 1-PTZ and the Corresponding Gas-Phase Dipole Moments[a]
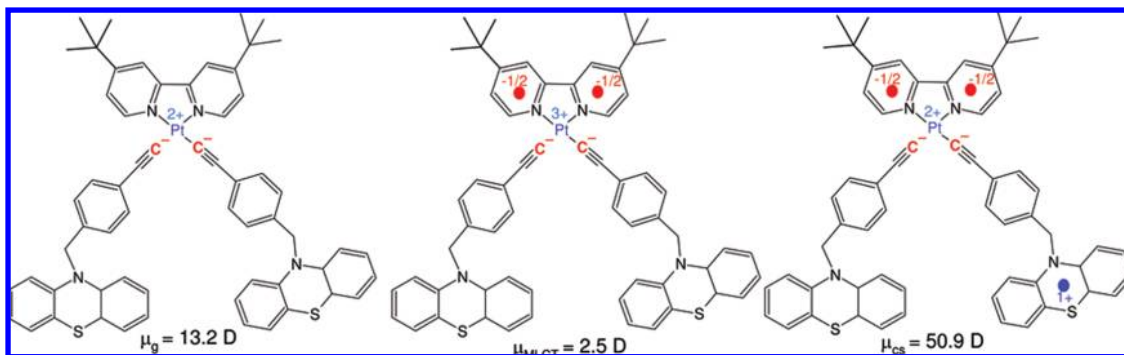
[a] Blue atoms or dots describe the positive charges of the value next to them; red atoms or dots similarly describe the negative charges. The dipole moments in different solvents, M_i, calculated for these states using these charge distributions are given in Table 3.
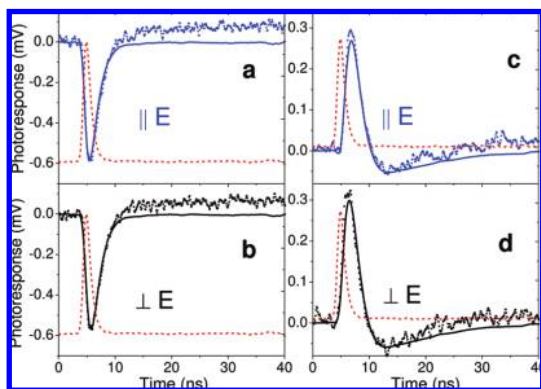

Figure 3. Photoresponses of **1** (**a** and **b**) and **1-PTZ** (**c** and **d**) in CH_2Cl_2 at room temperature excited at 420 nm with the light polarization parallel (left) and perpendicular (right) to the applied electric field of 700 V across a 0.79 mm gap. The dotted lines are the experimental photoresponses (at 50 μJ of absorbed energy for **1** and 4 μJ for **1-PTZ**), and the red dashed line is the laser pulse time profile. The solid lines are the simulated data fittings with the parameters listed in Tables 1 and 2. Discrepancies visible at longer time are due to photoionization of solutes and photoinjection of electrons from the electrodes that are often observed in such polar solvents and appear as a fast-rising continuous current.[34]

Figure 4. Photoresponses of **1** (**a** and **b**) and **1-PTZ** (**c** and **d**) in THF at room temperature excited at 420 nm with the light polarization parallel (left) and perpendicular (right) to the applied electric field of 700 V across a 0.79 mm gap. The dotted lines are the experimental photoresponses (scaled to 150 μJ of absorbed energy in all cases), and the red dashed line is the laser pulse time profile. The solid lines are the simulated data fittings with the parameters listed in Tables 1 and 2.

($\varepsilon = 8.93$) has opposite sign (see Figure 3) to that in toluene, indicating a much larger dipole moment for the CS state than the ground state. The parameters used to fit the PTDC photoresponse of **1-PTZ** in various solvents are summarized in Table 2. Because of a large difference between the excited- and ground-state dipole moments, the fit is almost insensitive to the value of the ground-state dipole moment, M_g, (similar to how the signal was almost insensitive to a small value of M_{MLCT} in toluene and was primarily defined by M_g), but it is sensitive to the choice of the charge separation time to PTZ, τ_{CS}. A simple qualitative observation suggests that τ_{CS} is not very short; otherwise, the signals for different light polarizations would differ more substantially than is experimentally observed. The best fit analysis suggest that $\tau_{CS} = 0.5 \pm 0.2$ ns and the charge recombination lifetime is $\tau_{CR} = 9 \pm 1$ ns. Because of a large RC time ($\tau_{RC} = 1.3$ ns in CH_2Cl_2), the rotation time can be only estimated from the fit as not exceeding 0.6 ns. The value in Table 2, $\tau_r = 0.4 \pm 0.1$ ns, was estimated from the viscosity and the hydrodynamic scaling based on that of **1-PTZ** in toluene.

As shown in Figure 4, the PTDC signal for **1-PTZ** in THF ($\varepsilon = 7.58$) has the most bizarre profile. The more complex photoresponse is attributed to rapid formation of ^{3}MLCT state (with the dipole moment close to zero), followed less rapidly
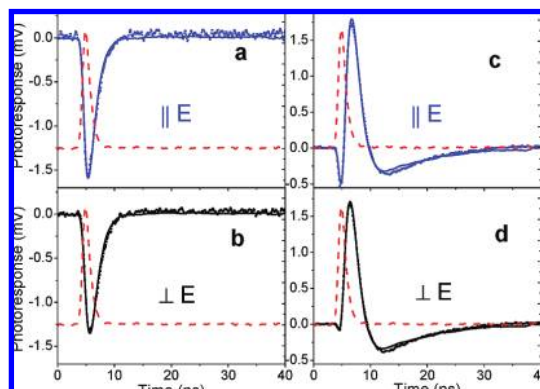
by appearance of the CS state with a large dipole moment oriented opposite to that of the ground state. The unusual appearance of the signal in THF, starting negative and doubly crossing zero, can only occur when all the following conditions are fulfilled: (a) the dipole moment of the CS state, M_{CS}, is oppositely oriented to that of the ground state, (b) the dipole moment of the CS state is larger in absolute value than that of the ground dtate, $M_{CS} > M_g$, and (c) both the rotational time, τ_r, and the charge separation time, τ_{CS}, are sufficiently long to allow the various steps to be resolved in time. In THF the CS state lifetime, τ_{CR}, is 8 ± 1 ns and corresponds to the dipole signal approaching zero at long times. The dipole signal profiles for both light polarizations in Figure 4 can be fit with the ground-state dipole moment, $M_g = 12 \pm 2$ D, and the CS dipole moment of $M_{CS} = 21 \pm 1$ D. Again, there is almost no dependence on the dipole moment of the MLCT state, M_{MLCT}, with minute preference toward slightly positive values, $M_{MLCT} = 2 \pm 2$ D. The best fit is obtained with the charge separation time $\tau_{CS} = 0.6 \pm 0.1$ ns. The rotation time value in Table 2, $\tau_r = 0.45 \pm 0.1$ ns, was estimated from the viscosity and the hydrodynamic volume scaling using that of **1-PTZ** in toluene.

It is surprising at first that, despite a small difference between the dielectric constants of THF and CH_2Cl_2, and very similar charge separation and charge recombination times for **1-PTZ** in these solvents, the dipole moments of the CS states in **1-PTZ**

Platinum(II) Diimine-Centered Triads

J. Phys. Chem. A, Vol. 113, No. 23, 2009 **6435**

TABLE 3: Dipole Moments M_i (including solvent contribution, M_{si}) Calculated for Different States and Hydrodynamic Volumes of 1-PTZ in Different Solvents

solvent	M_g (D) (μ_g = 13.2 D)[a]	M_{MLCT} (D) (μ_{MLCT} = 2.5 D)[a]	M_{CS} (D) (μ_{CS} = 50.9 D)[a]	ε	R_s (Å)[b]	η, mPa·s[c]	V, Å^{3d}
CH_2Cl_2	10.3	2.2	41.5	8.9	2.3	0.41	4000
THF	10.4	2.2	41.9	7.6	2.5	0.46	4300
toluene	11.4	2.3	45.4	2.4	2.8	0.56	4800

[a] The gas-phase dipole moments correspond to charges located as shown in Scheme 2. [b] Effective solvent radii used for calculating solvent volume in formula. [c] Solvent viscosity at 25 °C from ref30 [d] Hydrodynamic volume calculated as a solvent inaccessible volume.[28]
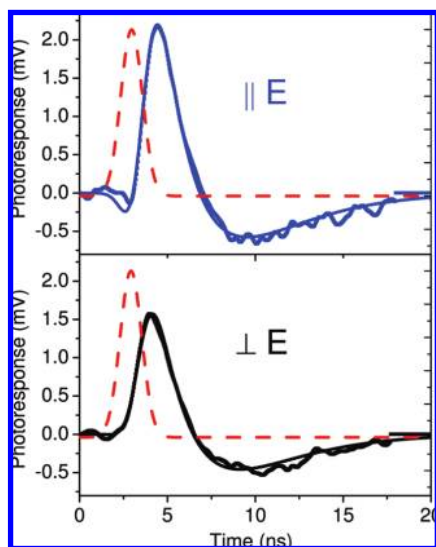

Figure 5. Photoresponses of **2-PTZ** in THF at room temperature excited at 450 nm with the light polarization parallel (left) and perpendicular (right) to the applied electric field of 700 V across a 0.32 mm gap. The dotted lines are the experimental photoresponses (scaled to 10 μJ of absorbed energy), and the red dashed line is the laser pulse time profile. The solid lines are the simulated data fittings with M_g = 15 D, M_{CS} = 42 D, and the lifetime is τ_{CR} = 2.7 ± 0.1 ns. See text for details.

are so dissimilar (M_{CS} = 21 and 44 D, respectively). The anticipated μ'_{CS} value can be determined by adding a separate pair of charges to make bpy$^-$ and PTZ$^+$, respectively, as shown in Scheme 2. With this charge arrangement, the gas phase value CS dipole moment is estimated to be $\mu_{CS} \sim 51$ D, which reduces to $M_{CS} \sim 45$ D in toluene and $M_{CS} \sim 42$ D in THF and CH_2Cl_2. The slightly larger experimentally measured value in CH_2Cl_2 can be attributed to a solvent-induced electric polarization caused by increasing reaction field and some conformational changes in the molecule, i.e., nuclear polarization. As pointed out above, limitations of the semicontinuum approximation in calculating the solvent contribution, m_s, might also be significant.

Nevertheless, the much smaller apparent value of M_{CS} for **1-PTZ** in THF suggests that, in this environment, the CS and ^{3}MLCT states are equilibrated, a condition achievable if (in THF) the states are nearly isoenergetic. Thus, the apparent value would correspond to a population-weighted average of dipole moments for the CS and ^{3}MLCT; see below.

With the equilibration interpretation in mind, another triad, **2-PTZ**, featuring a more electronegative bpy moiety and thus a more stable CS state, was examined; see Figure 5. Our expectation was that apparent value of M_{CS} would be dominated by contributions from the CS state. Experiments revealed that this is indeed the case. The dipole moment of the CS state for
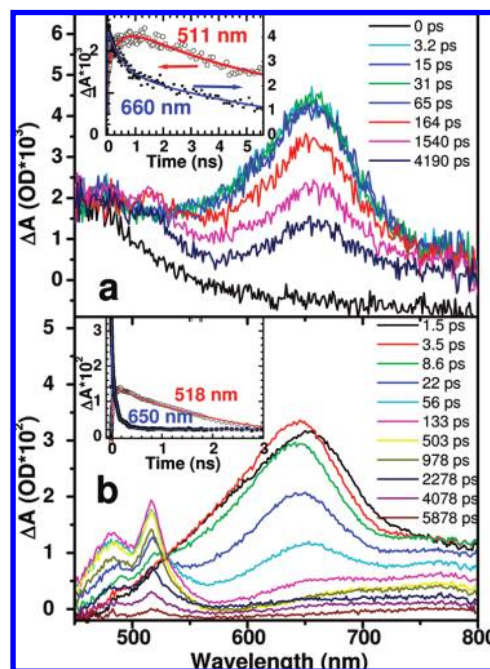

Figure 6. The transient absorption spectra for **1-PTZ** (a) and **2-PTZ** (b) in THF at room temperature upon excitation by the second harmonic of a Ti:Sapphire laser (415 nm). The time slices are listed in the spectra. The inset in part a shows the kinetic traces at 660 nm (^{3}MLCT absorption) and at 511 nm (PTZ radical cation), which were both fitted with the same τ_{CS} = 0.6 ± 0.1 ns and τ_{CR} = 8 ± 1 ns. The inset in part b shows the kinetic traces at 650 nm (^{3}MLCT absorption) and at 518 nm (PTZ radical cation).

2-PTZ in THF is M_{CS} = 42 ± 3 D, close to that of **1-PTZ** in CH_2Cl_2, and the lifetime is τ_{CR} = 2.7 ± 0.1 ns. The rotational time was scaled as 0.5 ns. Analyses of the transient absorption data for **1-PTZ** and **2-PTZ** in THF complement the dipole signal interpretation. Figure 6 shows their spectra at different time delays. A strong initial absorption feature at 660 nm for both molecules is due to the ^{3}MLCT state.[26] Absorption of PTZ$^+$ cation radical at 511 nm appears upon formation of the CS state. For **2-PTZ** the cation absorption grows in rapidly and concomitantly with decay of the ^{3}MLCT state. Indeed, the two time constants are identical, τ_{CS} = 80 ± 20 ps, and thus describe the charge separation time. Recombination to the ground state, monitored by disappearance of absorption at 511 nm, proceeds with τ_{CR} = 2.7 ± 0.1 ns, in agreement with the transient dipole measurements. Again, the situation with **1-PTZ** is more interesting. Even though the formation of PTZ$^+$ cation monitored at 511 nm appears within 0.6 ns (the same as in dipole signal formation), its intensity never grows to the full extent observed for **2-PTZ**. Both peaks, PTZ$^+$ at 511 nm and ^{3}MLCT at 660 nm, disappear with the same time constant of charge recombination, τ_{CR} = 8.0 ± 1.0 ns, which also agrees with the observed lifetime of CS state measured by PTDC.

The agreement between transient absorption and PTDC experiments in interpreting equilibrium between CS and ^{3}MLCT allows a deeper conclusion to be drawn. The dipole moment in THF can be treated as an average, $\langle M_{CS} \rangle$, between the dipole moments of the CS state, M_{CS}, and that of M_{MLCT}. The value of M_{CS} can be taken as that in CH_2Cl_2, where equilibrium is strongly biased toward the CS state. Since the charge separation time is longer than the rotation time, one can estimate:

6436 *J. Phys. Chem. A, Vol. 113, No. 23, 2009*

McGarrah et al.

$$\langle M_{CS} \rangle \sim n_{CS} M_{CS} + n_{MLCT} M_{MLCT}$$
$$= (k_{CS} M_{CS} + k_{-CS} M_{MLCT})/(k_{-CS} + k_{CS}) \quad (14)$$

where k_{CS} and k_{-CS} are the rates of charge separation and back recombination to the ^{3}MLCT state, respectively. Since $\langle M_{CS} \rangle$/$M_{CS} \sim 0.5$, the concentration of the ^{3}MLCT to CS states are approximately equal and $k_{CS} \sim k_{-CS}$.

Conclusions

Charge distribution and its evolution following photoexcitation in platinum(II) diimine triads have been characterized by the photoinduced transient displacement current technique. The ground-state dipole moment in **1** agrees well with a simple model where the charge of Pt(II) ion is compensated by the negative charges located on the neighboring carbons of the acetylides; the dipole moment slightly increases with solvent polarity, suggesting that the molecule is moderately polarizable in the ground state. The ^{3}MLCT excited state has a very small dipole moment. The dipole moments for the ground, ^{3}MLCT, and CS states in **1-PTZ** are in good agreement with elementary descriptions of charge distributions within these states as shown in Scheme 2. Population of the charge-separated (CS) state does not proceed in toluene but does occur in THF and CH_2Cl_2. The unusual PTDC photoresponse of **1-PTZ** in THF illustrates, to our knowledge, the only organometallic example of a charge-separated state in detectable equilibrium with an MLCT state. Consistent with the equilibration notion, the dynamics of charge transfer to and from PTZ are characterized by approximately equal time constant: each is ca. 0.6 ns. Charge transfer to PTZ in CH_2Cl_2 proceeds faster than in THF, while the back reaction is slowed, leaving the equilibrium heavily biased toward the CS state. The finding is supported by transient absorption studies.

References and Notes

(1) Wasielewski, M. R. *Chem. Rev.* **1992**, *92*, 435–461.
(2) Bignozzi, C. A.; Schoonover, J. R.; Scandola, F. *Prog. Inorg. Chem.* **1997**, *44*, 1–95.
(3) Chakraborty, S.; Wadas, T. J.; Hester, H.; Schmehl, R. H.; Eisenberg, R. *Inorg. Chem.* **2005**, *44*, 6865–6878.
(4) Smirnov, S. N.; Braun, C. L. *Rev. Sci. Instrum.* **1998**, *69*, 2875–2887.
(5) Smirnov, S. N.; Braun, C. L. *Chem. Phys. Lett.* **1994**, *217*, 167–172.
(6) Smirnov, S. N.; Braun, C. L. *J. Phys. Chem.* **1994**, *98*, 1953–1961.
(7) Mylon, S. E.; Smirnov, S. N.; Braun, C. L. *J. Phys. Chem.* **1998**, *102*, 6558–6564.
(8) Smirnov, S.; Vlassiouk, I.; Kutzki, O.; Wedel, M.; Montforts, F. P. *J. Am. Chem. Soc.* **2002**, *124*, 4212–4213.
(9) Vlassiouk, I.; Smirnov, S.; Kutzki, O.; Wedel, M.; Montforts, F. P. *J. Phys. Chem. A* **2002**, *106*, 8657–8666.
(10) Montforts, F.-P.; Vlassiouk, I.; Smirnov, S.; Wedel, M. *J. Porphyrins Phthalocyanines* **2003**, *7*, 651–666.
(11) Smirnov, S. N.; Liddell, P. A.; Vlassiouk, I. V.; Teslja, A.; Kuciauskas, D.; Braun, C. L.; Moore, A. L.; Moore, T. A.; Gust, D. *J. Phys. Chem. A* **2003**, *107*, 7567–7573.
(12) Smirnov, S. N.; Braun, C. L.; Greenfield, S. R.; Svec, W. A.; Wasielewski, M. R. *J. Phys. Chem.* **1996**, *100*, 12329–12336.
(13) Reference deleted by author.
(14) McGarrah, J. E.; Eisenberg, R. *Inorg. Chem.* **2003**, *42*, 4355–4365.
(15) Hissler, M.; Connick, W. B.; Geiger, D. K.; McGarrah, J. E.; Lipa, D.; Lachicotte, R. J.; Eisenberg, R. *Inorg. Chem.* **2000**, *39*, 447–457.
(16) Whittle, C. E.; Weinstein, J. A.; Goerge, M. W.; Schanze, K. S. *Inorg. Chem.* **2001**, *40*, 4053–4062.
(17) Chan, C.-W.; Cheng, L. K.; Che, C. M. *Coord. Chem. Rev.* **1994**, *132*, 87–97.
(18) James, S. L.; Younus, M.; Raithby, P. R.; Lewis, J. *J. Organomet. Chem.* **1997**, *543*, 233–235.
(19) Adams, C. J.; James, S. L.; Liu, X.; Raithby, P. R.; Yellowless, L. J. *J. Chem. Soc., Dalton Trans.* **2000**, 63–67.
(20) Connick, W. B.; Geiger, D.; Eisenberg, R. *Inorg. Chem.* **1999**, *38*, 3264–3265.
(21) Wadas, T. J.; Lachicotte, R. J.; Eisenberg, R. *Inorg. Chem.* **2003**, *42*, 3772–3778.
(22) Chan, S.-C.; Chan, M.-C.; Wang, Y.; Che, C.-M.; Chneung, K.-K.; Zhu, N. *Chem.—Eur. J.* **2001**, *7*, 4180–4184.
(23) Pomestenchenko, I. E.; Castellano, F. N. *J. Phys. Chem. A* **2004**, *108*, 3485–3492.
(24) Hua, F.; Castallano, F. N. *Inorg. Chem.* **2006**, *45*, 4304–4306.
(25) Castellano, F. N.; Pomestchenko, I. E.; Shikhova, E.; Hua, F.; Muro, M. L.; Rajapakese, N. *Coord. Chem. Rev.* **2006**, *250*, 1819–1828.
(26) Excitation into the ^{1}MLCT band leads to rapid formation of the ^{3}MLCT, within 200 ± 40 fs. In effect, the only excited species present on the timescale of the laser pulse (∼2 ns) is the ^{3}MLCT state: Danilov, E. O.; Pomestchenko, I. E.; Kinayyigit, S.; Gentili, P. L.; Hissler, M.; Ziessel, R.; Castellano, F. N. *J. Phys. Chem. A* **2005**, *109*, 2465–2471.
(27) Fleming, G. R.; Morris, J. M.; Robinson, G. W. *Chem. Phys.* **1976**, *17*, 91–100.
(28) Here the hydrodynamic volume is taken to equal the solvent-inaccessible volume evaluated by 'rolling' a 'solvent molecule' over the surface given by atoms in the molecule with their van der Waals radii from ref 29 solvent radii were taken to be 2.8 Å, 2.5 Å, and 2.3 Å, for toluene, THF, and CH_2Cl_2, respectively. Note that this volume is significantly larger than the van der Waals volume, by more than a factor of 5 in the case of toluene.
(29) Bondi, A. *J. Phys. Chem.* **1964**, *68*, 441–451.
(30) *Handbook of Organic Solvents*; Lide, D. R., Ed.; CRC Press: Boca Raton, FL, 1995.
(31) Kang, Y.; Lee, J.; Song, D.; Wang, S. *Dalton Trans.* **2003**, 3493–3499.
(32) A program written by Dr. Vlassiouk was used for calculating solvent contribution, M_{si}, to the total dipole moment $M_i = \mu_i + M_{si}$. Solvent accessible volume was evaluated by 'rolling' a 'solvent molecule' over the surface given by atoms in the molecule with their van der Waals radii from ref 29; solvent radii were taken to be 2.8 Å, 2.5 Å, and 2.3 Å, for toluene, THF, and CH_2Cl_2, respectively.
(33) Vanhelmont, F. W. M.; Johnson, R. C.; Hupp, J. T. *Inorg. Chem.* **2000**, *39*, 1814–1816.
(34) Findley, B. R.; Smirnov, S. N.; Braun, C. L. *J. Phys. Chem. A* **1998**, *102*, 6385–6389.